



Publisher homepage: www.universepg.com, ISSN: 2663-7529 (Online) & 2663-7510 (Print)

<https://doi.org/10.34104/ejmhs.022.024040>

European Journal of Medical and Health Sciences

Journal homepage: www.universepg.com/journal/ejmhs

European Journal of
Medical and
Health Sciences



A Comprehensive Review on the Diabetic Retinopathy, Glaucoma and Strabismus Detection Techniques Based on Machine Learning and Deep Learning

Md. Muntasir Kamal^{1*}, Md. Hachibul Islam Shanto¹, Mirza Mahmud Hossan¹, Md. Abul Hasnat¹, Sharmin Sultana¹, and Milon Biswas¹

¹Department of Computer Science Engineering, Bangladesh University of Business and Technology, Dhaka, Bangladesh.

*Corresponding author: muntasir3217@gmail.com (Md. Muntasir Kamal, Department of Computer Science Engineering, Bangladesh University of Business and Technology, Dhaka, Bangladesh).

ABSTRACT

Diabetes is a condition in which a person's body either does not respond to insulin supplied by their pancreas or does not create enough insulin. Diabetics are at a higher chance and risk of acquiring a variety of eye disorders over time. Early identification of eye diseases via an automated method has significant advantages over manual detection thanks to developments in machine learning techniques. Recently, some high research articles on the identification of eye diseases have been published. This paper will present a comprehensive survey of automated eye diseases detection systems which are Strabismus, Glaucoma, and Diabetic Retinopathy from a variety of perspectives, including (1) datasets that are available, (2) techniques of image preprocessing, and (3) deep learning models. The study offers a thorough overview of eye disease detection methods, including cutting-edge field methods, intending to provide vital insight into the research communities, all eye-related healthcare occupational, and diabetic patients.

Keywords: Strabismus, Glaucoma, Diabetic retinopathy, Convolutional neural network, and Deep learning.

INTRODUCTION:

Eye diseases comprise a group of eye disease combinations that includes Diabetic Retinopathy, Strabismus, Glaucoma, etc (Valverde *et al.*, 2019). All types of eye diseases are harmful to human beings. For affecting eye diseases there occurs blindness and loss of vision from 20-74 ages. According to WHO, around 2.2 Billion people are affected by different types of eye diseases. In this article, we will discuss DR, GL, and Strabismus. Diabetic Retinopathy is an eye disease. Damage to the bloodstream of the light-sensitive tissues at the optic nerve causes DR. In the backside of the eye, this retina is indeed a sensitive layer of the eye that converts lights into electric signals.

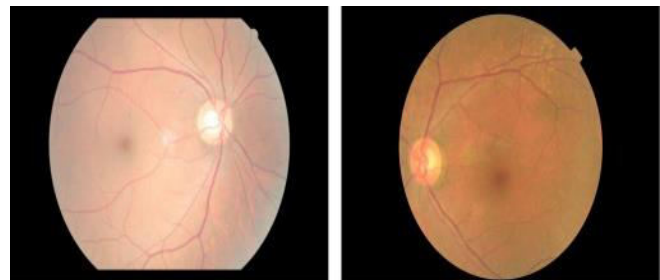


Fig. 1: Normal eyes fundus images.

In the backside of the eye, this retina is indeed a sensitive layer of the eye that converts lights into electric signals. To see the visual object, the brain decodes the electric signal. The retina needs a supply of blood constantly, which it receives through a tiny blood vessels network.

The major two stages of DR include - (i) Early DR, (ii) Advanced DR. Early DR is generally known as NPDR (non-proliferative diabetic retinopathy). In the early stage of DR, the retina's blood vessel walls are weakened. From the vessel walls, the Wendy lumps are protruded, occasionally leaking blood and fluid into the retina. Tissues inside the retina may expand, conducting white spots inside the retina. On the other hand, advanced DR is said PDR (proliferative diabetic retinopathy). In advanced DR, the damaged blood vessels prick the crystalline jelly that fills the center of the eye causing the improvement of odd blood vessels inside the retina. The pressure can increase in the orb because recently produced blood vessels break the normal flow of the fluid. This can damage the optic disk or nerve which carries images from the eye to the brain. The effects of DR are – gradually worsening vision, blurred vision, sudden vision loss eye pain or redness, etc (Azam *et al.*, 2020).

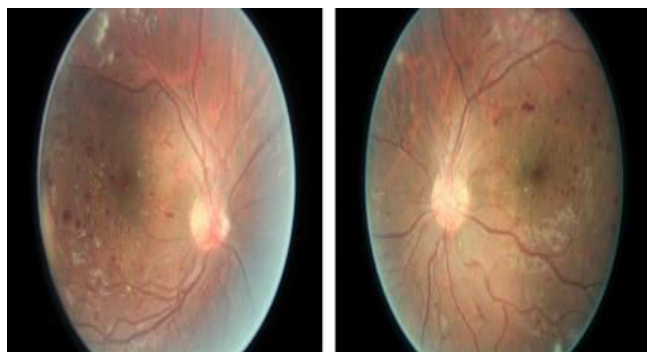


Fig. 2: Diabetic Retinopathy.

Another eye disease is Glaucoma. It's a condition of eye disease where the optic nerve is damaged. The nerve links the eyes to the human brain. When the eye's intraocular levels are high, the optic nerve suffers, It's the purpose for affecting glaucoma. The main sign of GL is a visual impairment. One of the most

common causes of blindness is GL. The signs and symptoms of glaucoma are – (i) intense eye pain (ii) red-eye, (iii) nausea and vomiting, (iv) a headache, (v) tenderness around the eyes, (vi) seeing rings around lights, (vii) blurred vision, etc. There are mainly two types of GL. They are - (i) open-angle (ii) angle-closure.

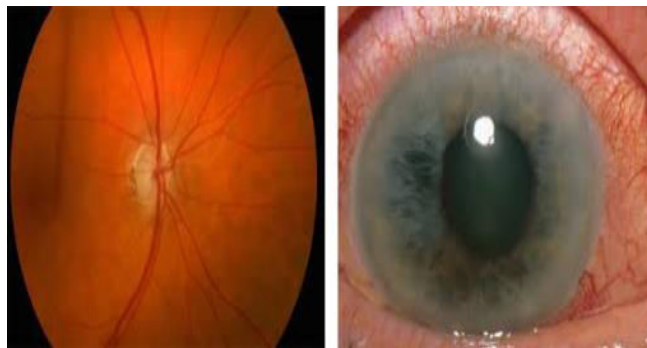


Fig. 3: Glaucoma.

Strabismus is another eye diseases condition where the eyes are not lined up with one another. In other words, we can say, one eye is turned in a direction that is completely different from another eye. In normal eye conditions, the six muscles control eye movement and point both eyes together (Khaleduzzaman *et al.*, 2021).

The problem in the functioning of these muscles or in the nerves that control these muscles is thought to be the cause of strabismus. The strabismus-affected patients can't control eye movement and can't keep normal ocular alignment. The most common signs and symptoms of strabismus are – (i) Double vision, (ii) Blurry vision, (iii) Difficulty in reading, (iv) Loss of depth perception, (v) weakness around the eyes. There are 4 categories strabismus which are – (i) esotropia, (ii) exotropia, (iii) hypertropia, (iv) hypotropia.



Fig. 4: Strabismus.

METHODOLOGY:

A well-organized selection is used to do research. First of all, we targeted a survey then we selected keyword-based papers on related work. After that we did a critical review of selected articles then the observation and discussion process is done on the articles. Finally, the conclusion is done. The below flowchart shows the research procedure.



Fig. 5: Diagram of our research method.

Selection of Articles:

We collected articles from 8 different databases considering our review target. The 8 databases are - (i)

IEEE Explore (ii) Science Direct (iii) DeepAI (iv) Springer (v) Academia (vi) SSRN (vii) Hindawi (viii) ACM. From them, we applied seven filtering methods to select our primary review target. The first filtering process is done for ML, DL, TL, image processing, image classification, diabetic retinal disease, diabetic eye disease, DR, GL, and Strabismus keywords. The second filtering method refers to the articles published from the year 2016 to 2021. The third filtering method is based on conferences and journals. To remove duplicate articles, we used the fourth filtering method. The fifth filtering method is based on articles title, abstract, introduction, and conclusion. The sixth filtering method is done by scanning references and citations. The final filtering method is quality assessment. The filtering method is shown in the figure below:

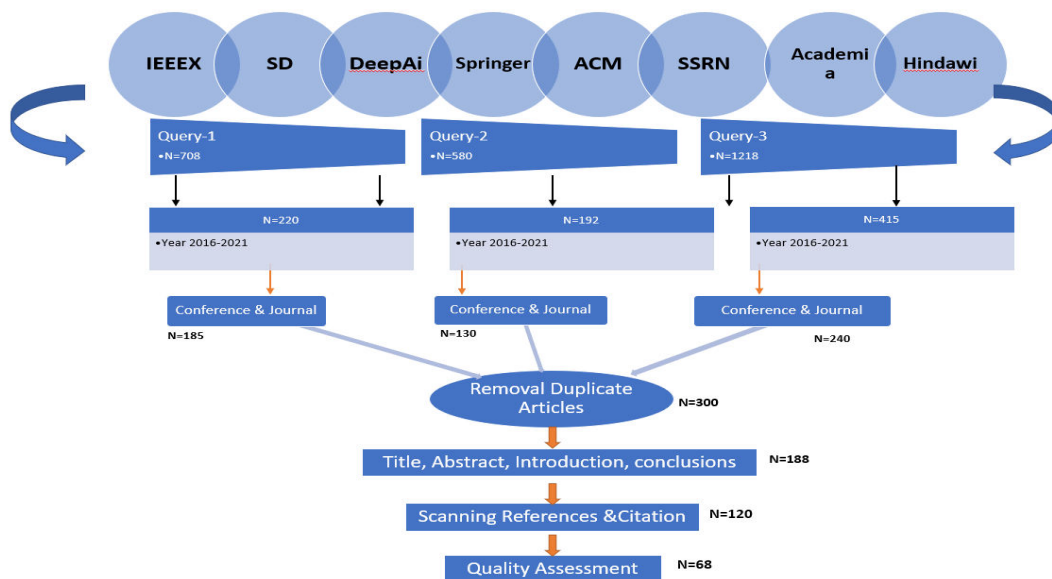


Fig. 6: Selection process of our articles.

Eye Diseases Data Sets

The articles we have selected, In those articles, the authors used public and private datasets. The datasets are from Cave, Kaggle, Eye Disease Dataset, Siblings DB, and Messidor (Zolkifli *et al.*, 2021), (Decencièrè *et al.*, 2014), (Jain, 2018; Almeida *et al.*, 2012). They are used for sample image data for training and testing. Authors (Zolkifli *et al.*, 2021) used Cave, Kaggle, Eye Disease Dataset, and SiblingsDB used for sample image data for research. Authors in (Gondal *et al.*, 2017; Gulshan *et al.*, 2016; Quelled *et al.*, 2017, Roy *et al.*, 2017; Li *et al.*, 2017; Grinsven *et al.*, 2016; Sayres *et al.*, 2019; Doshi *et al.*, 2016; Gargeya *et al.*, 2017;

Jiang *et al.*, 2017; Hajabdollahi *et al.*, 2019; Bir *et al.*, 2020; Yang *et al.*, 2017; Torre *et al.*, 2020; Torre *et al.*, 2020; Sisodia *et al.*, 2017) used Kaggle dataset and (Li *et al.*, 2017; Van Grinsven *et al.*, 2016; Umapathy *et al.*, 2019; Abbas *et al.*, 2017; Orlando *et al.*, 2018; Bahrami *et al.*, 2018; ZOLKIFLI *et al.*, 2021) used the dataset from Messidor (Decencièrè *et al.*, 2014). There are 88,702 images in the Kaggle dataset. In that, about 35,126 and 53,576 images are used for training and testing purposes. There are 1200 fundus images in Messidor (Decencièrè *et al.*, 2014), which is the most widely used dataset. The below **Table** shows information of selected articles datasets –

Table 1: Short form of various terms.

Full form	Short-form
Diabetic Retinopathy	DR
Glaucoma	GL
Deep Learning	DL
Machine Learning	ML
Transfer learning	TL
Convolutional neural network	CNN
proliferative diabetic retinopathy	PDR
Random Forest	RF
Support Vector Machine	SVM
Backpropagation Neural Network	BPNN
Gaussian Filter	GF
Illumination Correction	IC
Image Rotation	IR

Blood Vessel Segmentation	BVS
Grayscale Conversion	GSC
Augmentation	Au
Resize	Re
Contrast Enhancement	CE
Contrast Limited Adaptive Histogram Equalization	CLAHE
Region of Interest	ROI
Histogram Equalization	HE
Green Channel Extraction	GCE
Optical coherence tomography	OCT
Cross-validation	CV
Medical image analysis group	MIAG
Prevalence and Bias-Adjusted Fleiss' Kappa	PABAK
Diabetic Eye Disease	DED

Table 2: DR, GL, Strabismus datasets description.

Eye Disease	Dataset	Description	References
DR	Messidor	The dataset has 1200 fundus images. Among the 1200 images, 800 and 400 are with and without pupil dilation.	(Li <i>et al.</i> , 2017; Grinsven <i>et al.</i> , 2016; Abbas <i>et al.</i> , 2017; Orlando <i>et al.</i> , 2018; Bahrami <i>et al.</i> , 2018)
	Kaggle	The dataset consists of 88702 images where 35126 and 53576 images were used for training and testing.	(Zolkifli <i>et al.</i> , 2021; Gondal <i>et al.</i> , 2017; Gulshan <i>et al.</i> , 2016; Vaghefi <i>et al.</i> , 2020; Quellec <i>et al.</i> , 2017; Roy <i>et al.</i> , 2017; Li <i>et al.</i> , 2017; Grinsven <i>et al.</i> , 2016; Sayres <i>et al.</i> , 2019; Doshi <i>et al.</i> , 2016; Gargeya, <i>et al.</i> , 2017; Jiang <i>et al.</i> , 2017; Hajabdollahi <i>et al.</i> , 2019; Bir <i>et al.</i> , 2020; Yang <i>et al.</i> , 2017; Jain <i>et al.</i> , 2018; Almeida <i>et al.</i> , 2012; Torre <i>et al.</i> , 2020; Torre <i>et al.</i> , 2020; Sisodia <i>et al.</i> , 2017)
	Friedrich-Alexander University machine learning data	There are 522 healthy and 1021 diseased images. The images were increased then to get 1680 images. There were about 960 and 720 diseased and healthy images.	(Jain <i>et al.</i> , 2018)
	Deep DR	For the classification of DR, In the dataset consists of 2696 pictures which are from 748 patients.	(Zhang <i>et al.</i> , 2019)
GL	RIGA	There are three different sources in the dataset. Bin Rushed (There are 195 original images in the dataset those are marked by different six ophthalmologists total about 1365 images). MESSIDOR (The dataset contains 460 original photographs. Which are manually defined by six different ophthalmologists total of about 3220 images). Magrabi Eye Center (There are 95 original images in the dataset those are marked by different six ophthalmologists total about 665 images)	(Al Ghamdi <i>et al.</i> , 2019)

Strabismus	The tele strabismus dataset	In the dataset, there are 5685 images. For training purposes, 3409 images are used and for testing purposes, 2276 images are used. Among the training dataset, there are 2708 normal images and 701 strabismus images. On the other hand, the test dataset is consists of 1806 normal and 470 strabismus images.	(Al Ghamdi <i>et al.</i> , 2019)
	CAVE	There are 5880 images in the CAVE dataset. They are 56 different subjects ranging from 18 – 36 years old people. Among them 32 are males and 24 are females.	(Zolkifli <i>et al.</i> , 2021)
	Siblings DB	In the dataset, there exist 184(92 siblings pair) images of their anterior, profile, vacant, and chuckling faces. Among them profile images are 79 pairs and 56 images are of have chuckling vacant and profile pictures.	(Zolkifli <i>et al.</i> , 2021)
	Eye disease dataset	The Eye disease dataset is gained from Kaggle. There are 88702 images in the dataset. Where 35126 and 53576 images were used for training and testing.	(Zolkifli <i>et al.</i> , 2021)
	Private Strabismus dataset from ophthalmological office in Saint Louis	The dataset consists of 45 patient images. Five images from each patient and are divided into two classes strabismus and normal. Total 225 images in the dataset.	(de Oliveira Simoes <i>et al.</i> , 2019)

Image Preprocessin Techniques Used in Selected Articles

There are various image processing methods and techniques to visualize the images. For increasing the visualization of the images, the images are subjected to some pre-processing steps. When the images are more clear and bright then a network can gist more supreme features. In this section, we will discuss a brief statement about the techniques of image processing that are used by the authors and researchers. On the RGB color space, the Green channel provides better contrast and information compared to the other channels (Simon, 2019). Green channel separation extraction is appointed in most image pre-processing techniques (Simon, 2019). Contrast enhancement is another very known image processing technique. Its application raises the contrast on green channel images. To raise the image, contrast enhancement is devoted to the green channel. Usually, Revelation correctness is completed to raise the brightness and intensity of light of the image after contrast enhancement. The Gaussian filter method is used to smooth out the pictures. Gaussian filter is a noise removal filter. Another well-known method of image processing is image resizing. As an example,

the resizing methodology starts with image acquisition. It is done by the re-dimensioning of the original image from 2048 * 1536 to 205 * 154 pixels, where the original resolution is greater than 10 times the re-dimensional resolution (Almeida *et al.*, 2012).

The main objective of resizing is to minimize the computational cost of image processing. Feature extraction is a section of the dimensionality shortening procedure. In which, a set of strong data is separated and attenuated to major manageable groups. So, when you're ready to process it, it'll be a lot easier. If you have a large quantity of data, feature extraction comes in handy. Feature extraction reduces the amount of duplicated data in a data source. Image segmentation is the method of partitioning different image parts from the eye like the inner and outer portion of the eye, retina part of the eye, pupil diameter (Gupta *et al.*, 2014), eyelid, sclera, eyelashes, eyelid, and take asides all impertinent niceties to improve the efficiency. Irises are typically depicted as circles of inner and outer boundaries. These two circles should not be co-centric in most cases (Umesh *et al.*, 2016). The Table shows the image processing techniques in selected articles.

Table 3: Image processing techniques in selected articles.

Reference	GF	IC	IR	BVS	GSC	Au	Re	CE	CLAHE	ROI	HE	GEC
(Li et al., 2017)	X	X	X	X	X	✓	✓	X	✓	✓	X	✓
(Abbas et al., 2017), (Diaz-Pinto et al., 2019)	X	X	X	X	X	X	X	X	X	✓	X	X
(Orlando et al., 2018)	X	✓	X	✓	X	X	X	X	X	✓	X	✓
(Bahrami et al., 2018)	X	X	X	X	X	X	X	X	X	✓	X	X
(Vaghefi et al., 2020)	✓	X	X	X	X	X	✓	X	X	✓	X	X
(Quellec et al., 2017)	✓	X	X	X	X	✓	✓	X	X	X	X	X
(Van Grinsven et al., 2016)	✓	X	X	X	X	✓	✓	✓	X	X	X	X
(Gargeya et al., 2017)	X	X	X	X	X	✓	✓	X	X	X	X	X
(Jiang et al., 2017)	X	X	X	X	X	X	✓	X	X	X	✓	X
(Yang et al., 2017)	X	X	X	X	X	X	✓	X	✓	✓	X	X
(de La Torre et al., 2020)	X	X	X	X	X	✓	X	✓	X	X	✓	X
(Gargeya et al., 2017)	X	X	X	X	X	✓	✓	X	X	X	X	X

Eye Diseases Classification Techniques

Here, we will investigate the approaches which are Deep Learning-based for Eye diseases detection. In Deep Learning architecture the word "deep" mentions the depth of the layers. The classification processes are :

- 1) The annotated dataset is divided into training and testing data for DL architecture,
- 2) For quality enhancement, the dataset is by the use of image preprocessing techniques.
- 3) For features extraction and posterior classifications, the preprocess images are compiled into DL architecture.

Here previous layer output is used as input for the current layer in DL architecture and the previous layer output is processed and passed into the following layer. From the DL algorithm, many researchers used subsisting hyperparameters like CNN or VGG-16. The algorithms are used for improving classification accuracy.

Dlapproa Ches for Empliyng TL, New Network, and Combined DL ML

On the primary task, TL is used for the reuse of features that is learned by DL models and its adaptation to the secondary task. When the Neural Network Architecture is trained, TL is used to minimize the computational cost. In some events, to train a Neural Network when there is not enough data then the TL is beneficial. The arguments are launched from the former learning instead of random propagation. The primary layers become acquainted with gist the fundamental features like textures, edges, and so forth whereas the peak layers are earmarked more such as exudates and blood vessels. Consequently, inimage recognition applications TL is commonly adopted as initial features gifted are shared mindless to the task. From our all studies, some researchers propounded an aggregation of ML and DL classifiers. Based onarchitecturethe researchers used RF, SVM, and BPNN for detecting eye diseases. In this Table, Hyperparameter observed in selected articles are given –

Table 4: Hyperparameter observation.

References	Model	Image Size	Mini Batch Size	Epoch	Optimizers	Initial Learning Rate
(Quellec et al., 2017)	o_o	448 * 448	36	-	Adam	1 x 10 ⁻⁴
(Gondal et al., 2017)	o_o	512 * 512	-	150	Adam	1 x 10 ⁻²
(Phan et al., 2019)	ResNet152 DenseNet201,VGG19	512 * 512, 256 * 256	-	-	-	-
(Sayres et al., 2019)	InceptionV4	779 * 779	-	-	-	-
(Sharma et al., 2020)	CNN	256 * 256	15	200	Adam	1 x 10 ⁻⁵
(Li et al., 2017)	AlexNet	512 * 512	-	130	-	1 x 10 ⁻²

(Van Grinsven <i>et al.</i> , 2016)	OxfordNet	41 * 41	256	60	-	1×10^{-5}
(Asaoka <i>et al.</i> , 2019)	ResNet	224 * 224	64	-	SGD	1×10^{-3}
(Diaz-Pinto <i>et al.</i> , 2019)	VGG16, VGG19	224 * 224, 299 * 299	8	100	SGD	1×10^{-4}
(Gómez-Valverde <i>et al.</i> , 2019)	VGG19, RESNET50 GoogLeNet, DENET, Standard CNN	231 * 231, 231 * 231	32,64	100; 80; 25, 50	SGD	1×10^{-4}
(Ahn <i>et al.</i> , 2018)	InceptionV3	224 * 224	-	14	Gradient Descent	1×10^{-5}
(Sahlsten <i>et al.</i> , 2019)	InceptionV3	2095* 2095	15	-	-	-
(Jiang <i>et al.</i> , 2017)	CNN	224 * 224	-	600	-	1×10^{-2}
(Torre <i>et al.</i> , 2020)	CNN	128 * 128	-	250; 150; 70	Adam	1×10^{-3} , 1×10^{-4} , 1×10^{-5}
(Torre <i>et al.</i> , 2020)	CNN	512 * 512	15	300	Adam	$3 \times (1 \times 10^{-4})$
(Hemanth <i>et al.</i> , 2020)	CNN	64 * 64	-	20	Adam	1×10^{-5}
(Raghavendra <i>et al.</i> , 2018)	CNN	256 * 256	-	100	-	1×10^{-2} ; 1×10^{-3} ; 1×10^{-4}
(Ramamamy <i>et al.</i> , 2021)	NNET	224 * 224	-	-	-	-
(Zolkifli <i>et al.</i> , 2021)	R2018b	5184*3456 for cave. 4526*283 for Siblings DB	-	-	-	-
(Figueiredo <i>et al.</i> , 2021)	ResNet50			150		

DR

DR is a kind of retinopathy caused by diabetes. DR is the subject of numerous research papers. The system employed in (Tufail *et al.*, 2017), is Retinal pictures were manually graded using three ARIAS: iGradingM, Ret marker, and Eye Art, and processed using a standard national approach for DR screening. A reading center was resorted to for arbitration when ARIAS scores differed from manual grading. The screening performance (sensitivity, false-positive rate) and diagnostic accuracy (95 percent confidence intervals of screening-performance parameters) were determined in the research publication (Tufail *et al.*, 2017). The cost per appropriate screening outcome was calculated using economic analysis. The following are the ARIAS sensitivity point estimates (95 % confidence intervals) as a consequence of the experiment: Eye Art 94.7 % (94.2 % e95.2 %) for any retinopathy, 93.8 % (92.9 % e94.6 %) for referable retinopathy (human graded as ungradable, maculopathy or proliferative), and 99.6 % (97.0 % e99.9 %) for proliferative retinopathy; Ret marker 73.0 % (72.0 % e74.0 %) for all photos were assessed as having illness or being ungradable by iGradingM. The method was validated using 400 ret-

inal fundus pictures from the MESSIDOR database, yielding average values of 97 % accuracy, 94 % sensitivity (recall), 98 % specificity, 94 % precision, 94 % F Score, and 95 % t GMean for various performance evaluation metrics.

The suggested work (Saranya *et al.*, 2020) focuses on establishing a computer-aided diagnosis tool to detect and classify DR in its early stages, as well as employing Convolution Neural Net-works to grade non-proliferative DR from retinal fundus pictures (CNN). The methodology that is being suggested Upsampling or downsampling the data, optic disc segmentation, pre-processing images to make them model ready, and feeding pre-processed images to the CNN model for severity grading are the four stages involved. The method's limits are found in the photographs that are fed, as the categorization is heavily dependent on the quality of the images pro-vided. They achieved a result of 96 %sensitivity and 91 % accuracy. (Kumar *et al.*, 2020) reported an automated early DR diagnosis technique based on improved blood vessel and optic disc segmentation strategies. This study focused on red lesion features such as microaneurysms and hemorrhages to detect the early stages of DR using the DIA-

RETDB1 database. This enhanced model has a sensitivity of 87 % and a specificity of 93%. They present a DR model employing red lesion localization and a Convolution CNN classifier in this paper (Zago *et al.*, 2020). This model was developed using DIARETDB1 datasets and tested against a variety of databases, including MESSIDOR, it achieved 91% accuracy and 94% sensitivity. The disadvantage is that only red lesion features were evaluated for DR checking, and brilliant lesions were not taken into account.

GL

There is a good amount of research about GL. The researchers employed ResNet architecture then examined two datasets from different institutions (Asaoka *et al.*, 2019). To boost the data volume, they used the data augmentation approach, and the area under the receiver operating characteristic curve was used to discover their accuracy (AROC). Therefore, they obtained two outcomes: 94.8 % AROC in a supplemented dataset and 99.7% AROC in a dataset without augmentation. Using color fundus pictures and TL, they identified Optical coherence tomography in three dimensions (OCT) and GL in (An *et al.*, 2019). The model AUC was evaluated tenfold using cross-validation (CV). When five different CNN models were coupled with Random Forest, the CV AUC increased tenfold to 96.3 %. In (Diaz-Pinto *et al.*, 2019), five publicly available datasets were used by the researchers. They achieved a result in the sensitivity of 93.46%, specificity of 85.80%, AUC of 96.05%. In (Lu *et al.*, 2019), researchers classified glaucoma and non-glaucoma using the VGG network. Three separate ophthalmology centers in China provided them with VF samples. They got 82.6 % specificity, 87.6% accuracy, and 93.2 percent sensitivity. In (Al Ghamdi *et al.*, 2019) they used Semi-supervised and Supervised methods and achieved accuracy 92.4%, sensitivity 91.7%, and specificity of 93.3% in Semi-supervised. In Supervised accuracy 81.25%, sensitivity 74.2%, and specificity 86.3%.

In (Alghamdi *et al.*, 2021) provide a framework for automatically diagnosing GL that is based on three CNN models with distinct learning approaches in this research. They employed both labeled and unlabeled data to apply transfer and semi-supervised learning methods. To begin, the transfer learning model starts with a pre-trained CNN model that has been fine-tuned

using non-medical data. Second, a semi-supervised framework based on two different unsupervised approaches was trained and constructed utilizing labeled and unlabeled data. TCNN, SSCNN, and SSCNN-DAE are three models. They conducted trials utilizing two publicly available datasets, RIM-ONE and RIGA, to evaluate the GL diagnostic performance of their proposed CNN models. When comparing the classification accuracy of the various models of deep learning, it was observed that semi-supervised learning models outperformed transfer learning techniques. The SSCNN-DAE model had the greatest results, with an accuracy of 93.8 %, a sensitivity of 98.9 %, and a specificity of 90.5 %. (Gulshan *et al.*, 2016) in author by handcrafting feature-based segmentation in retinal pictures, an automatic computer-aided diagnostics (CADx) framework is constructed for diagnosing GL eye condition. It is proposed that Deep Learning and DBN (deep-belief network) be used to automate the detection of glaucoma. The four steps of the deep belief technique are (i) automatic detection, (ii) feature extraction, (iii) feature optimization, and (iv) classification. On average, the trial findings showed an accuracy of 98 %, sensitivity of 83 %, specificity of 97 percent, precision of 84 %, and recall of 86 %. Based on three-dimensional optical coherence tomography (OCT) data and color fundus pictures, this (An *et al.*, 2019) study attempted to build a machine learning-based method for GL diagnosis in open-angle GL patients. This study included 208 glaucomatous and 149 healthy eyes. A segmentation algorithm was used to create thickness and deviation maps. CNN transfer learning was also applied. Data augmentation is used to train CNN. A random forest (RF) was trained to classify the disc fundus images. The models were evaluated using 10-fold cross-validation (CV). Color fundus pictures had a 10-fold CV Area Under Curve of 0.940, RNFL thickness maps had a 10-fold CV Area Under Curve of 0.942, macular GCC thickness maps had a 10-fold CV Area Under Curve of 0.944, disc RNFL deviation maps had a 10-fold CV Area Under Curve of 0.949, and macular GCC deviation maps had a 10-fold CV Area Under Curve of 0.952. The 10-fold CV AUC was increased to 0.963 by RF merging the five different CNN models. At full, half, and quarter frequency scales, this study (Chaudhary *et al.*, 2021) proposes order zero and order one 2D-FBSE-EWT algorithm. Decomposition of a fundus image into rele-

vant sub-images is accomplished using these methods. Two approaches are employed to detect glaucoma from sub-images: (i) suggested method-1, a standard ML-based method, and (ii) suggested method-2, an ensemble method based on ResNet-50. The rim-one database of the medical image analysis group (MIAG) is used for proposed method- 1. To test the robustness, they employ three more databases: MIAG rim-one r3, Drishti-GS, and the original data-base. To create a huge database, all databases, including rim-one r1, r2, r3, Kristi-GS, and original, are integrated into proposed method-2. At full size, Method-1 produced the greatest results with one order 2D-FBSE-EWT. For databases r1, r2, and r12, the best accuracy is 98.21 percent using RF, 90 percent using SVM, and 95.51 percent using RF classifier in method 1. Approach 2 uses one order 2D-FBSE-EWT method-based sub-images at full frequency fusion ensemble's scale to achieve improved results, with accuracy, sensitivity, specificity, and Area Under Curve of ROC of 91.1 percent, 94.3 percent, 83.3 percent, and 0.96 percent, respectively.

Strabismus

Strabismus A good number of researchers have been studied and conducted for the automatic detection of Strabismus. The (Zolkifli *et al.*, 2021) system is conducted into 4 stages which are image acquisition, pre-processing, locating the glint on the irises and distance, and finally the classification for the strabismus types. To develop their algorithm, they used MATLAB (R2018b) image processing toolkit. For the CAVE, all the images are classified into normal individuals. Image 37 is the only hypertropia type found in the eye disease dataset while the other images are classified in esotropia types. In (Lu *et al.*, 2019) a deep neural network was utilized to analyze 5685 photos containing strabismus. For training and testing, 3409 and 2276 photos are used. There are 701 strabismus photos and 2708 normal images in the training dataset. The test dataset contains 470 strabismus photos and 1806 normal ones. They proposed a new method that is made up of two stages- (i) Eye segmentation is performed using R-FCN. (ii) To categorize the segmented eye areas as Strabismus or normal, a CNN is used. Result of first experiment: 1st CNN Network - Sensitivity-0.9330%, Specificity- 0.9617%, Accuracy- 0.9389%, AUC- 0.9865%. 2nd CNN Network - Sensitivity-0.95

24%, Specificity-0.9648%, Accuracy-0.9512%, AUC-0.9876%. In (Zolkifli *et al.*, 2021), The method used here - 1. Image Acquisition, 2. pre-processing, 3. Feature extraction that includes (i) Sobel Edge Detection (ii) Hough Transform. Using the Cave dataset, they achieved Avg Mean square error= 0.0003%, Avg Peak signal to noise ratio = 84.3540%. Using the Eye disease dataset, they achieved Avg Mean square error= 0.0012%, Avg Peak signal to noise ratio = 76.3595%. Using the Siblings DB dataset Avg Mean square error= 0.0004%, Avg Peak signal to noise ratio = 82.4973%. The method was broken down into six parts (Simoes *et al.*, 2019) including picture dataset acquisition, limb and eye localization, sclera segmentation and reconstruction, corners of the eyes, and classification in normal and strabismic patients. This approach is used to analyze a private strabismus dataset collected in a Sao Luis, Brazil, ophthalmology office. To develop their method, they used 225 images of 45 patients. YOLOv3 was used to locate the regions of the eyes and limbs, and data augmentation was employed to enlarge the training set in this stage. After this training set grew to 1280 images. They used U-net to perform scale segmentation. UBIRIS.v2 and SSRBC 2017 were the datasets utilized to train for the sclera segmentation stage. Hirschberg tests were employed in the five gaze positions DEXTRO, INFRA, LEVO, PP, and SUPRA to detect strabismus. The approach of PP and SUPRA placements produced the best results in identifying strabismic patients. The PP position had a sensitivity of 95.8%, a specificity of 100%, and a precision of 96.6%. 93 % of the youngsters (125/133) had at least one successful app measurement, according to (Cheng *et al.*, 2021). Six people were identified as having strabismus, including four exotropia (10Δ, 10Δ, 14Δ, and 18Δ), one continuous esotropia (25Δ), and one accommodating esotropia 14Δ). Based on the ROC curve, the appropriate threshold for the application to detect strabismus is 3.0, with the highest 83.0% sensitivity, 100% specificity, and 100% accuracy. One child with accommodative exotropia would have been missed by the app if this criterion had been used, three cases of intermittent exotropia would have been missed if traditional screening had been used. A total number of 38 patients with strabismus were included in the research (Yeh *et al.*, 2021). The APCT and the VR-based system's angle of ocular deviation had a good outstanding association (ICC= 0.897 (range:

0.810–0.945)). The 95 % confidence intervals were 11.32 PD. In the subgroup analysis, a significant difference between esotropia and exotropia was identified (p 0.001). In the esotropia group (mean = 4.65 PD), the amount of ocular deviation measured by the VR-based system was more than that measured by the APCT, but in the exotropia group (mean = 3.01

PD), the amount of ocular deviation indicated by the VR-based system was lower. The ICC was 0.962 (range: 0.902–0.986) in the esotropia group and 0.862 (range: 0.651–0.950) in the exotropia group. The 95 percent limits of agreement in the esotropia and exotropia groups were 6.62 PD and 11.25 PD each. The Table shows the result of DR, GL, and Strabismus –

Table 5: DR, GL and Strabismus results.

Eye Disease	Architecture / Classifier	Layers	Model	Ref.	Results
DR	o_OSolution		CNN	(Gondal et al., 2017)	Sensitivity = 93:6%, Specificity = 97:6%, Area Under Curve = 95:4%
	o_OSolution		CNN	(Quellec et al., 2017)	Area Under Curve = 95:4%
	ImageNet		CNN	(Roy et al., 2017)	Kappa Score = 86%
	U-Net		CNN	(Li et al., 2017)	Area Under Curve = 96%
	OxfordNet		CNN	(Grinsven et al., 2016)	Sensitivity = 91:90%, Specificity = 91:40%, Area Under Curve = 97:2%
	Inception-V4		CNN	(Sayres et al., 2019)	Accuracy = 88:4%
	AlexNet, GoogLe Net, VGGNets		CNN	(Li et al., 2017)	Sensitivity = 86:03%, Specificity = 97:11%, Area Under Curve = 98:34%, Accuracy = 92:01%
	Inception-V3		CNN	(Umopathy et al., 2019.)	Accuracy = 88:8%
	ResNet50		CNN	(Li et al., 2019)	Area Under Curve=92:6%, Accuracy = 96:3%
	AlexNet		CNN	(Harangi et al., 2019.)	Accuracy = 90:07%
	Softmax	8	CNN	(Hemanth et al., 2020)	Sensitivity = 94%, Specificity = 98%, Prec = 94%, FSc = 94%, GMean = 95%, Accuracy = 97%
	Softmax	29	CNN	(Doshi et al., 2016)	Kappa Score = 39:96%
	Decision Trees	6	CNN	(Gargeya et al., 2017)	Sensitivity = 93%, Specificity = 87%, Area Under Curve = 94%
	Softmax	28	CNN	(Gargeya et al., 2017)	Kappa Score = 75:4%, Prec = 88:20%, Sensitivity = 95%, Accuracy = 85%
	Softmax	17	CNN	(Jiang et al., 2017)	Accuracy = 75:70%
	Softmax	13	CNN	(Hajabdollahi et al., 2019)	Sensitivity = 95%, Specificity = 30%
	Softmax	16	CNN	(Bir et al., 2020)	Accuracy = 94:5%
	Softmax	10	CNN	(Yang et al., 2017)	Sensitivity = 95:90%, Specificity = 89:90% Area Under Curve = 96:87%
	Softmax	16	CNN	(Jain et al., 2018)	Sensitivity = 88:85%, Specificity = 96%, Accuracy = 91:92%
	Softmax	17	CNN	(de Almeda et al., 2012)	Sensitivity = 91:1%, Specificity = 90:8%
Softmax	16	CNN	(de La Torre et al., 2020)	Area Under Curve = 96:1%	
Softmax	3	CNN	(Abbas et al., 2017)	Sensitivity = 92.18%, Specificity = 94.50%, Area Under Curve = 92.4%	
RF	10	CNN	(Orlando et al., 2018)	Sensitivity = 97.21%, Area Under Curve = 93.47%	
SVM	3	DBN	(Arunkumar et al., 2017)	Sensitivity = 79.32%, Specificity = 97.89%, Accuracy = 96.73%	
GL	ResNet		CNN	(Asaoka et al., 2019)	Area Under Curve =99.7%
	VGG-19		CNN	(An et al., 2019)	Area Under Curve = 96:3%

	VGG-16,VGG-19, Inception-V3, ResNet50, Xception		CNN	(Diaz-Pinto <i>et al.</i> , 2019)	Sensitivity = 93:46%, Specificity = 85:80%, Area Under Curve = 96:05%
	VGG		CNN	(Lu <i>et al.</i> , 2019)	Sensitivity = 82:6%, Specificity = 93:2%, Accuracy = 87:6%
	VGG16		CNN	(Al Ghamdi <i>et al.</i> , 2019)	Sensitivity = 91:7%, Specificity = 93:3%, Accuracy = 92:4%
	VGG19, ResNet152, DenseNet201		CNN	(Phan <i>et al.</i> , 2019)	Area Under Curve =90%
	VGG-19		CNN	(Gómez-Valverde <i>et al.</i> , 2019)	Sensitivity = 87:01%, Specificity = 89:01%, Area Under Curve = 94%
	Inception-V3		CNN	(Ahn <i>et al.</i> , 2018)	Area Under Curve = 92:2%; Area Under Curve = 88:6%; Area Under Curve = 87:9%
	Softmax	18	CNN	(Raghavendra <i>et al.</i> , 2018)	Sensitivity = 98%, Specificity = 98.3%, Accuracy = 98.13%
	Softmax	6	CNN	(Pal <i>et al.</i> , 2018,)	Area Under Curve = 92.3%
	Softmax	6	CNN	(Sharma <i>et al.</i> , 2020)	Sensitivity = 96%, Specificity = 84%, Accuracy = 90%
	Softmax	12	CNN	(Singh <i>et al.</i> , 2020)	Area Under Curve = 8.31%, 88.7%
	RF	23	CNN	(Nazir <i>et al.</i> , 2020)	Sensitivity = 85%, Specificity = 90.8%, Accuracy = 88.2%
Strabi-smus	R-FCN		CNN	(Lu <i>et al.</i> , 2019)	1 st CNN Network – Sensitivity =0.9330% Specificity =0.9617% Area Under Curve =0.9865%. Accuracy =0.9389%
	R-FCN		CNN	(Lu <i>et al.</i> , 2019)	2nd CNN Network – Sensitivity =0.9524%, Specificity =0.9648%, Area Under Curve =0.9876%, Accuracy =0.9512%
			CNN	(Cheng <i>et al.</i> , 2021)	Sensitivity = 83.0%, Specificity = 76.5%.
	ResNet-18, U-Net		CNN	(de Oliveira Simoes <i>et al.</i> , 2019)	Sensitivity =95.8%, Specificity =100% Accuracy =96.6%

Another Table is given below that provides us information on which articles have used which type of results –

Table 6: Result types used in selected articles.

References	Babak	PPV	Prev	FSc	Kappa Score	Specificity	Sensitivity	Area Under Curve	Accuracy	GMean
(Gondal <i>et al.</i> , 2017), (Van Grinsven <i>et al.</i> , 2016; Gargeya, <i>et al.</i> , 2017; Yang <i>et al.</i> , 2017; Abbas <i>et al.</i> , 2017; Diaz-Pinto <i>et al.</i> , 2019; Gómez-Valverde <i>et al.</i> , 2019)	X	X	X	X	X	✓	✓	✓	X	X
(Jain <i>et al.</i> , 2018, Arunkumar <i>et al.</i> , 2017; Lu <i>et al.</i> , 2019; Al Ghamdi <i>et al.</i> , 2019; Raghavendra <i>et al.</i> , 2018; Sharma <i>et</i>	X	X	X	X	X	✓	✓	X	✓	X

(al., 2020; Nazir et al., 2020; de Oliveira Simoes et al., 2019)										
(Quellec et al., 2017; Li et al., 2017; La Torre et al., 2020; Asaoka et al., 2019; An et al., 2019; Phan et al., 2019; Ahn et al., 2018; Pal et al., 2018; Singh et al., 2020)	X	X	X	X	X	X	X	✓	X	X
(Sayres et al., 2019; Umapathy et al., 2019; Harangi et al., 2019; Jiang et al., 2017; Bir et al., 2020)	X	X	X	X	X	X	X	X	✓	X
(Roy et al., 2017; Doshi et al., 2016)	X	X	X	X	✓	X	X	X	X	X
(Li et al., 2017)	X	X	X	X	X	✓	✓	✓	✓	X
(Li et al., 2019)	X	X	X	X	X	X	X	✓	✓	X
(Hemanth et al., 2020)	X	X	✓	✓	X	✓	✓	X	✓	✓
(Gargeya et al., 2017)	X	X	✓	✓	X	X	✓	X	✓	X
(Hajabdollahi et al., 2019); (de Almeida et al., 2012).	X	X	X	X	X	✓	✓	X	X	X
(Orlando et al., 2018)	X	X	X	X	X	X	✓	✓	X	X
(Lu et al., 2019)	X	X	X	X	X	✓	✓	✓	✓	X

Selected Articles Models Strength and Weakness Table

The Table shows us the strength, weaknesses, accuracy of top-1 and top-5, parameters, and the depth of selected articles models.

Table 7: The Table shows us the strength, weakness.

Models	Accuracy of Top-1	Accuracy of Top-5	Parameters	Depth	Strength	Weakness
ResNet50	0.769	0.921	25,636,712	-	It reduces the vanishing-gradient problem, the total number of parameters, Strengthens feature propagation, encourages feature reuse.	One major weakness seems to be that the deeper network takes weeks of training before it can be used in real-world scenarios.
ResNet152	0.766	0.931	60,419,944	-	A huge number of networks can be trained easily without increasing the training error percentage.	Not defined yet.
VGG16	0.713	0.901	138,357,544	23	It's a great building block for learning purposes and easy to implement.	It's very slow to train.
VGG19	0.713	0.900	143,667,240	26	It's better performance than the VGG16 model.	It takes more memory.
AlexNet	0.6330	0.8460	62378344	8	AlexNet allows multi GPU training so bigger models can be trained here easily and it also helps to reduce	The model is not very deep and It doesn't do a good job with color

					training time.	photos.
GoogleNet	0.7480	0.922	23000000	22	It trains faster than VGG models and takes less memory space.	Not defined yet.
DenseNet201	0.773	0.936	20,242,984	201	It reduces the parameters, vanishes gradient problems, etc.	Not defined yet.
Inception v3	0.779	0.937	23,851,784	48	Compared to its contemporaries Inception v3 can achieve the lowest error rates.	-
Inception v4	0.80	0.95	43,00,0000	22	The architecture is simplified using more inception modules than inception v3.	-

Research GAP

We have studied more than 70 articles here. There are various study gaps that academics have neglected to fill in prior DED studies. They need to increase the effectiveness of different eye diseases detection. We addressed some of the issues that are given here:

Thriving Stronger DL models in medical imaging, DL has a very good contribution and disease diagnosis. However, it is tough to create more effective deep neural networks. A key solution is that the computational power can be increased by increasing the network capacity but there exists a chance of over-fitting. Creating an object-based model is another solution. Training on Minimum Data for learning, the DL software was employed by a very good amount of retinal images. When the dataset is few the DL doesn't provide the expected result with good accuracy. For that, there are available 2 solutions. The first is to make use of the length of enhancement methods where shifting, cropping, color building, and rotation are included. Another is to retrieve training data by employing feeble learning algorithms. Corresponding DL architecture for Medical Imaging Most of the DL, there are used different TL frameworks like AlexNet, GoogleNet, ResNet, VGGNet, etc. Generally, TL frameworks are created for the objects like flowers, animals, and so much more. So these architectures are not suitable enough for medical pictures. A new TL can be created that specializes in learning relevant medical images. Integrating TL and Cloud Computing Hereafter, to detect Eye diseases from the images of the retinal fundus the neural networks and cloud computing may be associated. For example, people from different communities could use their mobile phone cameras to capture the eye images individually. Then these images could be transmitted to the cloud computing system where the eye diseases detection system is created.

Finally, the system will identify the eye diseases and show the result to the patient.

CONCLUSION:

The survey paper provides an extensive overview of different eye diseases detection techniques which are Strabismus, DR, and GL. To acquire this goal, we conducted an appropriate comprehensive review of different publications. After selecting the final relevant publications, the study has been analyzed from the view of (i) Dataset, (ii) Image processing techniques, and (iii) method employed for classification. We categorized the survey into three eye diseases parts which are Strabismus, DR, and GL. The survey includes different articles where TL, DL, and ML approaches are adopted. We also find out some limitations from different articles here. At first, we shrink down the review which was conducted from January 2016 to June 2021. Then based on DL approaches, because of their state of art performance we limited the review. Finally, we concentrated on different keyword collections which helped us to provide a veil of eye diseases area. In the future, we hope that our research will be expanded more based on recent publications.

ACKNOWLEDGEMENT:

First and foremost, I acknowledge Allah's grace because it would not have been possible without it. In addition, I would like to express my gratitude to the co-authors and respected professors of the Bangladesh University of Business and Technology (BUBT) Department of Computer Science and Engineering for supervising me and giving us the necessary assistance to complete the research.

CONFLICTS OF INTEREST:

There are no conflicts of interest to be disclosed by any of the authors.

REFERENCES:

- 1) Abbas, Q., Fondon, I., Jiménez, (2017). Automatic recognition of severity level for diagnosis of diabetic retinopathy using deep visual features. *Medical & biological engineering & computing*, **55**(11), 1959-1974. <https://link.springer.com/article/10.1007/s11517-017-1638-6>
- 2) Ahn, J. M., Kim, S., Ahn, K. S., (2018). A deep learning model for the detection of both advanced and early glaucoma using fundus photography. *PloS one*, **13**(11), e0207982. <https://doi.org/10.1371/journal.pone.0211579>
- 3) Alghamdi, M., & Abdel-Mottaleb, M. (2021). A Comparative Study of Deep Learning Models for Diagnosing Glaucoma From Fundus Images. *IEEE Access*, **9**, 23894-23906. <https://doi.org/10.1109/ACCESS.2021.3056641>
- 4) Al Ghamdi, M., Li, M., & Abou Shousha, M. (2019). Semi-supervised transfer learning for convolutional neural networks for glaucoma detection. In *ICASSP 2019-2019 IEEE International Conference on Acoustics, Speech and Signal Processing* (pp. 3812-3816). *IEEE*. <https://doi.org/10.1109/ICASSP.2019.8682915>
- 5) An, G., Omodaka, K., Hashimoto, K., Tsuda, S., (2019). Glaucoma diagnosis with machine learning based on optical coherence tomography and color fundus images. *J. of healthcare engineering*, 2019. <https://doi.org/10.1155/2019/4061313>
- 6) Arunkumar, R., & Karthigaikumar, P. (2017). Multi-retinal disease classification by reduced deep learning features. *Neural Computing and Applications*, **28**(2), 329-334.
- 7) Asaoka, R., Tanito, M., Shibata, N., (2019). Validation of a deep learning model to screen for glaucoma using images from different fundus cameras and data augmentation. *Ophthalmology Glaucoma*, **2**(4), 224-231. <https://doi.org/10.1016/j.ogla.2019.03.008>
- 8) Azam MS, Rahman A, Iqbal SMHS, and Ahmed MT. (2020). Prediction of liver diseases by using few machine learning based approaches, *Aust. J. Eng. Innov. Technol.*, **2**(5), 85-90. <https://doi.org/10.34104/ajeit.020.085090>
- 9) Bahrami, M., & Sajedi, H. (2018). Prediction of diabetic retinopathy based on a committee of random forests. *International Journal of Intelligent Machines and Robotics*, **1**(2), 133-139.
- 10) Bhaskaranand, M., Ramachandra, C., Bhat, S., (2019). The value of automated diabetic retinopathy screening with the EyeArt system: a study of more than 100,000 consecutive encounters from people with diabetes. *Diabetes technology & therapeutics*, **21**(11), 635-643. <https://doi.org/10.1089/dia.2019.0164>
- 11) Bir, P., & Balas, V. E. (2020). A Review on Medical Image Analysis with Convolutional Neural Networks. In *2020 IEEE International Conference on Computing, Power and Communication Technologies* (pp. 870-876). *IEEE*. <https://doi.org/10.1109/GUCON48875.2020.9231203>
- 12) Chaudhary, P. K., & Pachori, R. B. (2021). Automatic diagnosis of glaucoma using two-dimensional Fourier-Bessel series expansion based empirical wavelet transform. *Biomedical Signal Processing and Control*, **64**, 102237. <https://doi.org/10.1016/j.bspc.2020.102237>
- 13) Cheng, W., Lynn, M. H., Pundlik, S., (2021). A smartphone ocular alignment measurement app in school screening for strabismus. *BMC ophthalmology*, **21**(1), 1-10.
- 14) Decencière, E., Zhang, X., Lay, B., (2014). Feedback on a publicly distributed image database: the Messidor database. *Image Analysis & Stereology*, **33**(3), 231-234. <https://www.ias-iss.org/ojs/IAS/article/view/1155>
- 15) de Almeida, J. D. S., Silva, A. C., de Paiva, A. C., (2012). Computational methodology for automatic detection of strabismus in digital images through Hirschberg test. *Computers in biology and medicine*, **42**(1), 135-146. <https://doi.org/10.1016/j.compbiomed.2011.11.001>
- 16) de Figueiredo, L. A., Dias, J. V. P., Polati, M., (2021). Strabismus and Artificial Intelligence App: Optimizing Diagnostic and Accuracy. *Translational Vision Science & Technol.*, **10**(7), 22-22. <https://doi.org/10.1167/tvst.10.7.22>
- 17) de La Torre, J., Valls, A., & Puig, D. (2020). A deep learning interpretable classifier for diabetic retinopathy disease grading. *Neurocom.*, **396**, 465-476. <https://doi.org/10.1016/j.neucom.2018.07.102>
- 18) de Oliveira Simoes, T., Souza, J. C., de Almeida, (2019). Automatic Ocular Alignment Evaluation

- for Strabismus Detection Using U-NET and Res Net Networks. In *2019 8th Brazilian Conference on Intelligent Systems* (pp. 239-244). *IEEE*.
<https://doi.org/10.1109/BRACIS.2019.00050>
- 19) Diaz-Pinto, A., Morales, S., Naranjo, V., (2019). CNNs for automatic glaucoma assessment using fundus images: an extensive validation. *Biomedical engineering online*, **18**(1), 1-19.
- 20) Doshi, D., Shenoy, A., & Gharpure, P. (2016). Diabetic retinopathy detection using deep neural networks. In *2016 International Conference on Computing, Analytics and Security Trends* (p. 261-266). *IEEE*.
<https://doi.org/10.1109/CAST.2016.7914977>
- 21) Gargeya, R., & Leng, T. (2017). Automated identification of diabetic retinopathy using deep learning. *Ophthalmology*, **124**(7), 962-969.
<https://doi.org/10.1016/j.ophtha.2017.02.008>
- 22) Gómez-Valverde, J. J., Antón, A., Fatti, G., (2019). Automatic glaucoma classification using color fundus images based on convolutional neural networks and transfer learning. *Bio-medical optics express*, **10**(2), 892-913.
- 23) Gondal, W. M., Köhler, J. M., Grzeszick, R., (2017). Weakly-supervised localization of diabetic retinopathy lesions in retinal fundus images. In *2017 IEEE international conference on image processing (ICIP)* (pp. 2069-2073). *IEEE*.
<https://doi.org/10.1109/ICIP.2017.8296646>.
- 24) Gulshan, V., Peng, L., Stumpe, M. (2016). Development and validation of a deep learning algorithm for detection of diabetic retinopathy in retinal fundus photographs. *Jama*, **316**(22), 2402-2410. <https://doi.org/10.1001/jama.2016.17216>.
- 25) Gupta, S., & Gagneja, A. (2014). Proposed iris recognition algorithm through image acquisition technique. *International J. of Advanced Research in Computer Science and Software Engineering*, **4**(2), 269-270.
- 26) Hajabdollahi, M., Esfandiarpour, R., Najarian, K., (2019). Hierarchical pruning for simplification of convolutional neural networks in diabetic retinopathy classification. In *2019 41st Annual International Conference of the IEEE Engineering in Medicine and Biology Society (EMBC)* (pp. 970-973). *IEEE*.
<https://doi.org/10.1109/EMBC.2019.8857769>
- 27) Harangi, B., Toth, J., Baran, A., & Hajdu, A. (2019). Automatic screening of fundus images using a combination of convolutional neural network and handcrafted features. In *2019 41st Annual International Conference of the IEEE Engineering in Medicine and Biology Society (EMBC)* (pp. 2699-2702). *IEEE*.
<https://doi.org/10.1109/EMBC.2019.8857073>
- 28) Hemanth, D. J., Deperlioglu, O., & Kose, U. (2020). An enhanced diabetic retinopathy detection and classification approach using deep convolutional neural network. *Neural Computing and Applications*, **32**(3), 707-721.
- 29) Jain, L., Murthy, H. S., Patel, C., & Bansal, D. (2018). Retinal eye disease detection using deep learning. In *2018 14th International Conference on Information Processing* (p1-6). *IEEE*.
<https://doi.org/10.1109/ICINPRO43533.2018.9096838>
- 30) Jiang, Y., Wu, H., & Dong, J. (2017). Automatic screening of diabetic retinopathy images with convolution neural network based on caffe framework. In *Proceedings of the 1st Intern. Conf. on Medical and Health Informatics 2017* (pp. 90-94). <https://doi.org/10.1145/3107514.3107523>
- 31) Khaleduzzaman K, Mahmud MH, and Podder PK. (2021). Detection and implementation of blood group and Hb level by image processing techniques. *Aust. J. Eng. Innov. Technol.*, **3**(5), 73-81. <https://doi.org/10.34104/ajeit.021.073081>
- 32) Kumar, S., Adarsh, A., Kumar, B., & Singh, A. K. (2020). An automated early diabetic retinopathy detection through improved blood vessel and optic disc segmentation. *Optics & Laser Technology*, **121**, 105815.
<https://doi.org/10.1016/j.optlastec.2019.105815>
- 33) Li, G., Zheng, S., & Li, X. (2017). Exudate detection in fundus images via convolutional neural network. In *International Forum on Digital TV and Wireless Multimedia Communications* (pp. 193-202). Springer, Singapore.
https://link.springer.com/chapter/10.1007/978-981-10-8108-8_18
- 34) Li, X., Liu, W., & Wang, T. (2017). Convolutional neural networks based transfer learning for diabetic retinopathy fundus image classification. In *2017 10th international congress on*

- image and signal processing, biomedical engineering and informatics* (pp. 1-11). *IEEE*.
<https://doi.org/10.1109/CISP-BMEI.2017.8301998>
- 35) Li, X., Hu, X., Yu, L., Zhu, L., (2019). CANet: cross-disease attention network for joint diabetic retinopathy and diabetic macular edema grading. *IEEE transact. on medical imaging*, **39**(5), 1483-1493. <https://doi.org/10.1109/TMI.2019.2951844>
- 36) Lu, J., Feng, J., Fan, Z., Huang, L., (2019). Automated strabismus detection based on deep neural networks for telemedicine application. *Knowledge-based systems*. **13**.
- 37) Nazir, T., Irtaza, A., Javed, A., (2020). Retinal image analysis for diabetes-based eye disease detection using deep learning. *Appl. Sci.*, **10**(18), 6185. <https://doi.org/10.3390/app10186185>
- 38) Orlando, J. I., Prokofyeva, E., Del Fresno, M., (2018). An ensemble deep learning based approach for red lesion detection in fundus images. *Computer methods and programs in biomedicine*, **153**, 115-127.
<https://doi.org/10.1016/j.cmpb.2017.10.017>
- 39) Pal, A., Moorthy, M. R., & Shahina, A. (2018). G-eyenet: A convolutional autoencoding classifier framework for the detection of glaucoma from retinal fundus images. In *2018 25th IEEE international conference on image processing (ICIP)* (pp. 2775-2779). *IEEE*.
<https://doi.org/10.1109/ICIP.2018.8451029>
- 40) Patil, N., Patil, P. N., & Rao, P. V. (2021). Convolution neural network and deep-belief network (DBN) based automatic detection and diagnosis of Glaucoma. *Multimedia Tools and Applications*, **80**(19), 29481-29495.
<https://link.springer.com/article/10.1007/s11042-021-11087-5>
- 41) Phan, S., Satoh, S. I., Yoda, Y., & Oshika, T. (2019). Evaluation of deep convolutional neural networks for glaucoma detection. *Japanese j. of ophthalmology*, **63**(3), 276-283.
<https://link.springer.com/article/10.1007/s10384-019-00659-6>
- 42) Quellec, G., Charrière, K., Boudi, Y., (2017). Deep image mining for diabetic retinopathy screening. *Medical image analysis*, **39**, 178-193.
<https://doi.org/10.1016/j.media.2017.04.012>
- 43) Raghavendra, U., Fujita, H., Bhandary, S. V., (2018). Deep convolution neural network for accurate diagnosis of glaucoma using digital fundus images. *Information Sciences*, **441**, 41-49.
<https://doi.org/10.1016/j.ins.2018.01.051>
- 44) Ramasamy, L. K., Kadry, S., & Damaševičius, R. (2021). Detection of diabetic retinopathy using a fusion of textural and ridgelet features of retinal images and sequential minimal optimization classifier. *PeerJ computer science*, **7**.
- 45) Roy, P., Cao, K., Sedai, S., (2017). A novel hybrid approach for severity assessment of diabetic retinopathy in colour fundus images. In *2017 IEEE 14th International Symposium on Biomedical Imaging* (pp. 1078-1082). *IEEE*.
<https://doi.org/10.1109/ISBI.2017.7950703>.
- 46) Sahlsten, J., Jaskari, J., Kivinen, J., (2019). Deep learning fundus image analysis for diabetic retinopathy and macular edema grading. *Scientific reports*, **9**(1), 1-11.
<https://www.nature.com/articles/s41598-019-47181-w>
- 47) Saranya, P., & Prabakaran, S. (2020). Automatic detection of non-proliferative diabetic retinopathy in retinal fundus images using convolution neural network. *Journal of Ambient Intelligence and Humanized Computing*, 1-10.
<https://link.springer.com/article/10.1007/s12652-020-02518-6>
- 48) Sayres, R., Taly, A., Blumer, K., (2019). Using a deep learning algorithm and integrated gradients explanation to assist grading for diabetic retinopathy. *Ophthalmology*, **126**(4), 552-564.
<https://doi.org/10.1016/j.ophtha.2018.11.016>
- 49) Sharma, A., Agrawal, M., Roy, S. D., & Gupta, V. (2020). Automatic glaucoma diagnosis in digital fundus images using deep CNNs. In *Advances in Computational Intelligence Techniques* (pp. 37-52). *Springer*.
<https://doi.org/10.1109/ISPCC48220.2019.8988512>
- 50) Simon, S. (2019). Retinal Image Enhancement and Eye Disease Identification. In *proceedings of the International Conference on Systems, Energy & Environment (ICSEE)*.
https://papers.ssrn.com/sol3/Papers.cfm?abstract_id=3445915

- 51) Singh, L. K., & Garg, H. (2020). Automated glaucoma type identification using machine learning or deep learning techniques. In *Advancement of Machine Intelligence in Interactive Medical Image Analysis* (pp. 241-263). Springer. https://link.springer.com/chapter/10.1007/978-981-15-1100-4_12
- 52) Sisodia, D. S., Nair, S., & Khobragade, P. (2017). Diabetic retinal fundus images: Pre-processing and feature extraction for early detection of diabetic retinopathy. *Biomedical and Pharmacology Journal*, 10(2), 615-626. <https://dx.doi.org/10.13005/bpj/1148>
- 53) Tufail, A., Rudisill, C., Egan, C., Kapetanakis, V. V., (2017). Automated diabetic retinopathy image assessment software: diagnostic accuracy and cost-effectiveness compared with human graders. *Ophthalmology*, 124(3), 343-351. <https://doi.org/10.1016/j.ophtha.2016.11.014>
- 54) Umopathy, A., Sreenivasan, A., Nairy, D. S., (2019). Image Processing, Textural Feature Extraction and Transfer Learning based detection of Diabetic Retinopathy. In *Proceedings of the 2019 9th International Conference on Bioscience, Biochemistry and Bioinform.* (pp. 17-21). <https://doi.org/10.1109/ACCESS.2020.3015258>
- 55) Umesh, L., Mrunalini, M., & Shinde, S. (2016). Review of image processing and machine learning techniques for eye disease detection and classification. *International Research Journal of Engineering and Technology*, 3(3), 547-551.
- 56) Van Grinsven, M. J., van Ginneken, B., Hoyng, (2016). Fast convolutional neural network training using selective data sampling: Application to hemorrhage detection in color fundus images. *IEEE transact. on med. imag.*, 35(5), 1273-1284. <https://dx.doi.org/10.1109/TMI.2016.2526689>
- 57) Yang, Y., Li, T., & Zhang, W. (2017). Lesion detection and grading of diabetic retinopathy via two-stages deep convolutional neural networks. In *International Conference on Medical Image Computing and Computer-Assisted Intervention* (pp. 533-540). Springer, Cham. https://link.springer.com/chapter/10.1007/978-3-319-66179-7_61
- 58) Yeh, P. H., Liu, C. H., Sun, M. H., (2021). To measure the amount of ocular deviation in strabismus patients with an eye-tracking virtual reality headset. *BMC ophthalmology*, 21(1), 1-8. <https://bmcophthalmol.biomedcentral.com/articles/10.1186/s12886-021-02016-z>
- 59) Zago, G. T., Andreão, R. V., Dorizzi, B., (2020). Diabetic retinopathy detection using red lesion localization and convolutional neural networks. *Com. in biology and medicine*, 116, 103537. <https://doi.org/10.1016/j.combiomed.2019.103537>
- 60) Zhang, W., Zhong, J., Yang, S., Gao, Z., Hu, J., (2019). Automated identification and grading system of diabetic retinopathy using deep neural networks. *Knowledge-Based Systems*, 175, 12-25. <https://doi.org/10.1016/j.knosys.2019.03.016>
- 61) Zolkifli, N. S., Nazari, A., Akir, R. M., & Vajravelu, A. (2021). Range Detection of Strabismus based on the Distance and Coordinates of the Iris. *International J. of Advanced Computer Systems and Software Engineering*, 2(1), 23-29.
- 62) Zolkifli, N. S., & Nazari, A. (2020). Tracing of Strabismus Detection Using Hough Transform. In *2020 IEEE Student Conference on Research and Development* (pp. 313-318). IEEE. <https://doi.org/10.1109/SCOReD50371.2020.9250949>

Citation: Kamal MM, Shanto MHI, Hossan MM, Hasnat MA, Sultana S, and Biswas M. (2022). A comprehensive review on the diabetic retinopathy, glaucoma and strabismus detection techniques based on machine learning and deep learning. *Eur. J. Med. Health Sci.*, 4(2), 24-40.

<https://doi.org/10.34104/ejmhs.022.024040> 